

NTIS HC 84.75

X-322-72-153
PREPRINT

NASA TM X- 66072

HEAT PIPE INVESTIGATIONS

(NASA-TM-X-66072) HEAT PIPE INVESTIGATIONS
 J. P. Marshburn (NASA) May 1972 53 p CSCL
 20M N73-11967
 G3/33 Unclas
 46609

JAMES P. MARSHBURN



MAY 1972



GODDARD SPACE FLIGHT CENTER
GREENBELT, MARYLAND

Reproduced by
**NATIONAL TECHNICAL
 INFORMATION SERVICE**
 U S Department of Commerce
 Springfield VA 22151

X-322-72-153
Preprint

HEAT PIPE INVESTIGATIONS

James P. Marshburn
Test and Evaluation Division

May 1972

Goddard Space Flight Center
Greenbelt, Maryland

PRECEDING PAGE BLANK NOT FILMED

HEAT PIPE INVESTIGATIONS

James P. Marshburn
Test and Evaluation Division

ABSTRACT

The OAO-C spacecraft has three circular heat pipes, each of a different internal design, located in the space between the spacecraft structural tube and the experiment tube, which are designed to isothermize the structure. Two of the pipes are used to transport high heat loads, and the third is for low heat loads.

The test problems discussed deal with the charging of the pipes, modifications, the mobile tilt table, the position indicator, and the heat input mechanisms. The final results showed that the techniques used were adequate for thermal-vacuum testing of heat pipes.

Preceding page blank

SUMMARY

The heat pipe is becoming one of the most valuable tools of the heat transfer engineer. This report presents an introduction to the basic characteristics of heat pipes, their method of functioning, the analytical equations used to gage the heat-transfer capabilities, and the results obtained from thermal-vacuum tests of the heat pipes for the Orbiting Astronomical Observatory spacecraft.

The sections on the selection of fluids, pipe materials, and wick materials indicate the logic used in the design of the heat pipes. The test results indicate the value of research and of performance predictions, and demonstrate the actual performance of the pipes. The test results are sufficiently accurate to prove the value of heat pipes for use in spacecraft and in equipment used on the ground.

CONTENTS

	<u>Page</u>
ABSTRACT	v
SUMMARY	vi
INTRODUCTION	1
HEAT PIPE DESIGN	3
Choice of Fluid	4
Compatibility	4
Latent Heat of Vaporization	4
Vapor Pressure	4
Wetability	5
Viscosity	7
Liquid Transport Factor	7
Choice of Container Material	9
Material	9
Power Density	9
External and Internal Forces	10
Choice of Wicking Device	10
Method of Charging a Heat Pipe	14
HEAT PIPE OPERATION	15
GOVERNING ANALYTICAL EQUATIONS	19
Pressure Gradient Equations	19
Capillary Pumping Pressure	20
Liquid Pressure Gradient	21
Vapor Pressure Gradient	23

CONTENTS - (continued)

	<u>Page</u>
Equations of Motion, Continuity, and Heat Transfer	25
Equation of Motion	25
Analytical Determination of ΔP	26
Boundary Conditions and Mass Flow Rates	29
Heat Transfer	30
Thermal Gradients	30
Flow Limitations: Entrainment	31
TEST CONFIGURATION	33
TEST RESULTS AND CONSIDERATIONS	37
Performance Requirements	37
Basic Test Philosophy and Goals	37
Test Results	38
Long Periods for Temperature Stabilization	38
Higher Delta Temperatures	38
Effects of Tilt	38
Burnout and Repriming	38
Cool-out and Overheating	40
Effects of Environment	41
REFERENCES	45

ILLUSTRATIONS

<u>Figure</u>		<u>Page</u>
1	Heat Pipe Used in the Orbiting Astronomical Observatory	3
2	Capillary Attraction (Rise of Liquid in Capillary Tube) and Wetting Angle	6
3	Complete Wetting of Tube when Wetting Angle $\theta = 0$ Degree	6
4	Liquid Transport Factor (Figure of Merit) for Various Liquids	8
5	Cross Sections of Various Types of Wicking Devices	11
6	Detailed Views of Artery Wicking Device	12
7	Wickless Heat Pipe	13
8	Heat Pipe Circulation and Pressure Diagrams	16
9	Heat Pipe Steady-operation Pressure Terms	19
10	Heat Pipe Vapor-liquid Interface	27
11	Vapor Velocity Profile within a Heat Pipe	28
12	Test Configuration: Heat Pipe Mounted on Tilt Table	33
13	Thermal-vacuum Chamber Setup	34
14	Locations of Heaters, Condensers, and Thermocouples	35

TABLES

<u>Table</u>		<u>Page</u>
1	Flight-heater Data (Chamber Walls at -40° C)	39
2	Test-heater Data (Chamber Walls at -40° C)	41
3	Flight-heater Data (Chamber Walls at 0° C)	42
4	Flight-heater Data (Chamber Walls at $+20^{\circ}$ C)	43

INTRODUCTION

A heat pipe is a device which efficiently transfers heat by means of fluid evaporation, mass heat transport, and then condensation to a fluid again, to provide an isothermal region along the pipe length. The heat pipe principle was first described by Gaugler (Ref. 1) in 1942, but was overlooked until 1963, when Grover (Ref. 2) investigated in detail the principles and the possible space applications.

Although heat pipes have been employed in recently-launched satellites, such as the Applications Technology Satellite-E (1969), Package Attitude Control (1969), Orbiting Astronomical Observatory-B (OAO-B, 1970), and in OAO-C (scheduled for a 1972 launch), the questions as to how to test the heat pipe units on the ground, and how to extrapolate the results to the zero-gravity flight conditions, have not been completely resolved. For this reason a study has been performed to determine the state of the art and to develop a program of meaningful tests for the heat pipes in a 1-G environment. This study was based on the analytics used to design the heat pipes and on a long series of experiments and tests on the pipes.

PRECEDING PAGE BLANK NOT FILMED

HEAT PIPE DESIGN

The heat pipe is basically a thin-walled tube which contains a heat-transporting fluid and a wick or wicking device to provide for movement of the liquid by capillary attraction. As used in the Orbiting Astronomical Observatory, and illustrated in figure 1, each of three heat pipes are tubes of 1.27 cm (one-half inch) diameter, with closed ends, bent in the form of a torus of 1.19 m (46.9-inch) diameter. These heat pipes are placed in the annulus formed by the central experiment tube and the spacecraft structural cavity, and surround an experimental telescope; they aid in keeping local sections of the instrument at approximately the same temperature, within $\pm 3^{\circ}\text{C}$, and aid in the isothermalization of the entire spacecraft.

In the basic design of a heat pipe, the first consideration is choice of the fluid which will be used, in order to operate within a specified thermal range. Then the tube or container and the type of wicking device can be designed, since the three are closely related and the tube and wick must match the requirements of the fluid.

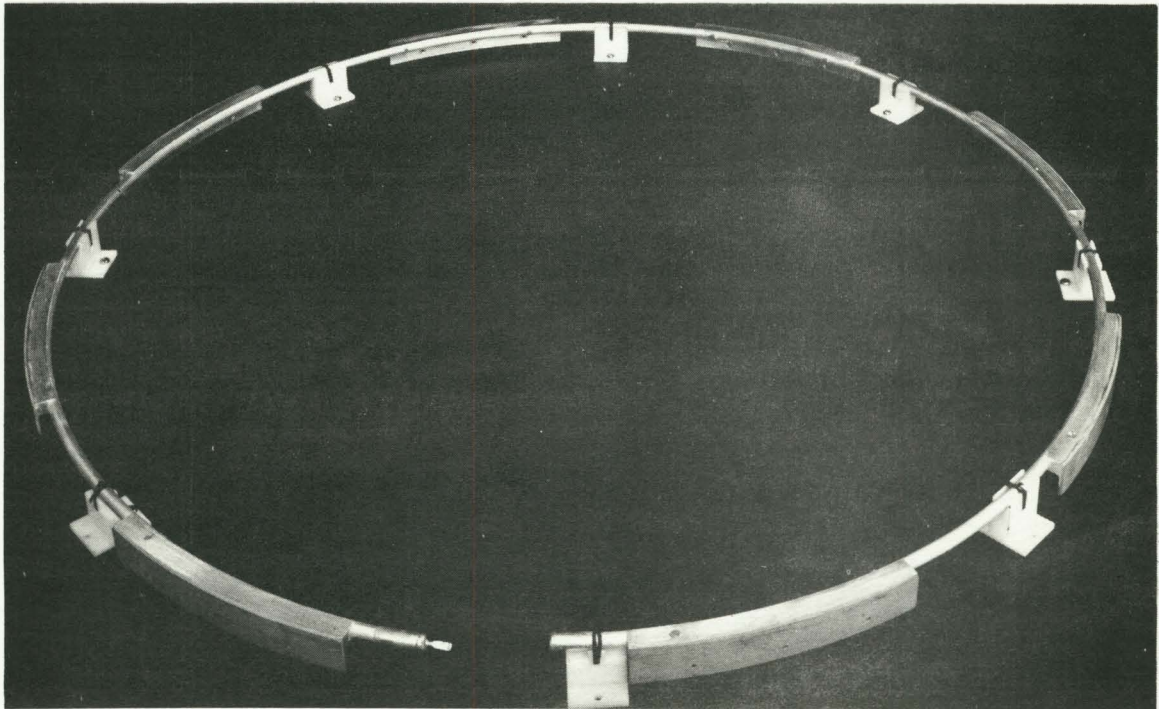


Figure 1. Heat Pipe Used in the Orbiting Astronomical Observatory

Preceding page blank

Choice of Fluid

The basic choice of a working fluid depends upon many factors, but for OAO-C and for most near-Earth satellites and deep-space probes the required thermal operating limits constitute the No. 1 parameter. These limits are in general -80°C to $+60^{\circ}\text{C}$. Other factors which must be considered in the selection of the working fluid are as follows:

1. Compatibility with other materials in the pipe and spacecraft;
2. High latent heat of vaporization;
3. Low vapor pressure;
4. Wetability, and
5. Low liquid viscosity.

Compatibility. For prolonged operating lifetime the working fluid must be compatible chemically with its wick and container (Refs. 3, 4), and sometimes with the spacecraft. In the case of the OAO-B heat pipes, an additional restriction was placed upon the choice of fluid, in that the fluid had to be compatible with the optical systems on the spacecraft. This requirement was made to ensure the safety of the optical systems in the event that a meteoroid were to puncture a heat pipe, which would cause the fluid to come into contact with the internal and external systems on the spacecraft. Based on this consideration one of the freons was selected for the OAO-B heat pipes. This fluid also provided a low internal vapor pressure, which in turn permitted minimum wall thickness and minimum weight. Anhydrous ammonia was selected for the later OAO-C heat pipes, because ammonia can carry more heat than the freons, and allows the heat pipe to function better.

Latent Heat of Vaporization. Latent heat of vaporization, h_{fg} , is the additional quantity of heat required to convert a liquid to a gas once the liquid has reached its boiling temperature. The values, on a per gas basis, are directly proportional to pressure and inversely proportional to temperature. The desirability of having a high h_{fg} is directly related to the maximum heat which can be transferred by a heat pipe. This is due to the fact that the heat transfer limit of any heat pipe is equal to the product of its mass flow rate and the latent heat of vaporization of the liquid used.

Vapor Pressure. Low vapor pressure is desirable, since the tube wall thickness is directly related to the internal pressure, because of safety factors. During its qualification testing one of the heat pipes for the Applications

Technology Satellite-F exploded, due to a combination of high internal vapor pressure and extreme wall thinness. Since that pipe was known to be thin, as determined by ultrasonic measurements, the proper precautions had been taken and the explosion caused no damage. However, the result of that test points up the necessity of having low vapor pressure, which prolongs the lifetime of a heat pipe.

Wetability. In order for a heat pipe to function properly, reducing the hot spots or thermal gradients, the liquid must wet thoroughly the wick and the containing vessel. This wetting ability is directly proportional to the cosine of the wetting angle. Figures 2 and 3 indicate a static arrangement for determining the wetting angle, θ , and the capillary pull, ΔP_c . When $\theta = 0$ degree, the pipe is said to be completely wet, and when $\theta = 90$ degrees, the pipe is dry. It is virtually impossible to determine this parameter in a flowing system. For this reason heat pipe designers usually calculate how much fluid is required to completely soak the heat pipe internal structural walls and wick, and load the pipe at a prescribed temperature with this amount of fluid, plus or minus five to 10 percent.

For the static arrangement shown in figure 2, the capillary pull, ΔP_c , is defined as the limit where the weight of the fluid column equals the gravitational force, or $\Delta P_c = \rho g h$ for this case. The height of the liquid in the capillary tube, h , is a variable, and can be raised or lowered depending upon the design of the wicking structure. Because most fluids entering the tube will form a concave surface, extending farther up the sides of the tube than at the center, as in a glass of water, the tube can be dry only when $\theta = 90$ degrees.

Complete wetability, $\theta \cong 0$ degree, as shown in figure 3, is more difficult to visualize. As the radius of curvature, r_c , shrinks, the fluid must extend higher up the walls of the tube until a limiting case is reached, where r_c equals approximately one-half the tube diameter. In this case the fluid assumes a profile parallel to the sides of the tube, which yields the limit of $\theta \cong 0$ degree. Theory predicts that this occurs most readily in low and zero-G environments, and this is proven by free-fall experiments (Refs. 5, 6). Among the various fluids which can be used, Mercury is a notable exception, in that it does not extend up the tube and does not wet the tube. The reason for this is that it has high surface tension.

Surface tension forces allow liquids, when in free fall, to form spheroidal shapes. This occurs because surface tension forces tend to form minimum surface areas for all fluids. In general this minimum-surface ability increases for all fluids as the temperature drops below ambient; i.e., the surface tension forces increase for all fluids, but vary in strength depending upon the fluid used. In a thermal-vacuum test of one of the pipes for the OAO-C spacecraft,

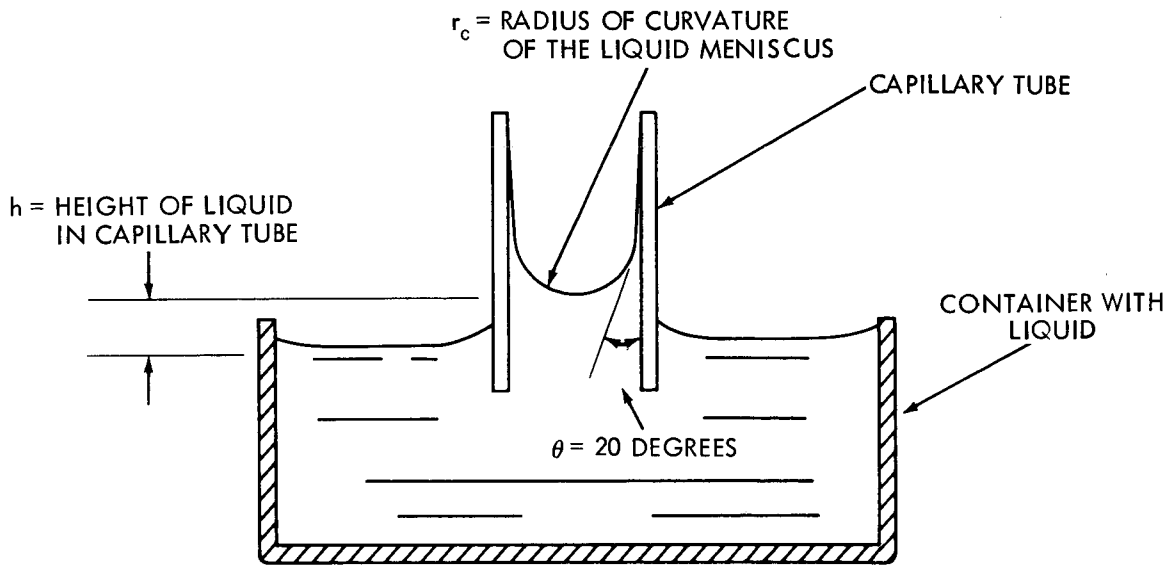


Figure 2. Capillary Attraction (Rise of Liquid in Capillary Tube) and Wetting Angle

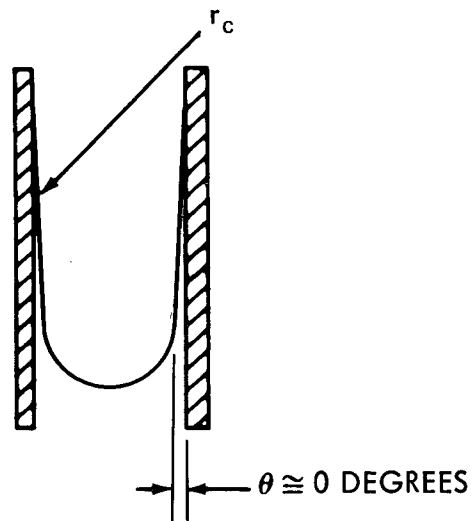


Figure 3. Complete Wetting of Tube when Wetting Angle $\theta = 0$ Degree

charged with anhydrous ammonia, it was proven in a low temperature test at -45°C (Ref. 24) that high values of surface tension caused the liquid to collect in the condenser sections, the cold sections of the heat pipe, and this created an out-of-tolerance condition in reference to the test specification. Further tests indicated that anhydrous ammonia can be used successfully in the -40° to $+50^{\circ}\text{C}$ temperature range when the proper materials are used for tube and wicking structure.

Viscosity. Low liquid viscosity allows the fluid to flow more freely in the return-flow portions of the pipe, producing less drag, and this in turn provides better heat transport, preventing high temperature gradients along the length of the pipe.

Liquid Transport Factor. A standard way of analyzing the capacity of a liquid to transport heat is based upon a lumped parameter of all the fluid properties. This is sometimes called a figure of merit, but more recently it is referred to as the liquid transport factor, N_f (Ref. 7). This is given as

$$N_f = \frac{\sigma \rho_f h_{fg}}{\mu_f}$$

where

σ = fluid surface tension,

ρ_f = fluid density,

h_{fg} = latent heat of vaporization, and

μ_f = fluid viscosity.

A graph of the liquid transport factor, covering a wide thermal band, is given in figure 4 for various working fluids. This graph indicates the temperature range in which each fluid can be used. However, for the use of any given fluid, experience dictates that a careful analysis of each property embodied in N_f is warranted. For example, a high value of latent heat of vaporization, high fluid density, and high fluid surface tension would usually be desirable, in conjunction with low viscosity. However, if the fluid density is sufficiently high, the drag forces may inhibit the flow of the fluid, resulting in unsatisfactory thermal gradients. Therefore, in choosing any heat pipe fluid, almost all conceivable parameters must be considered.

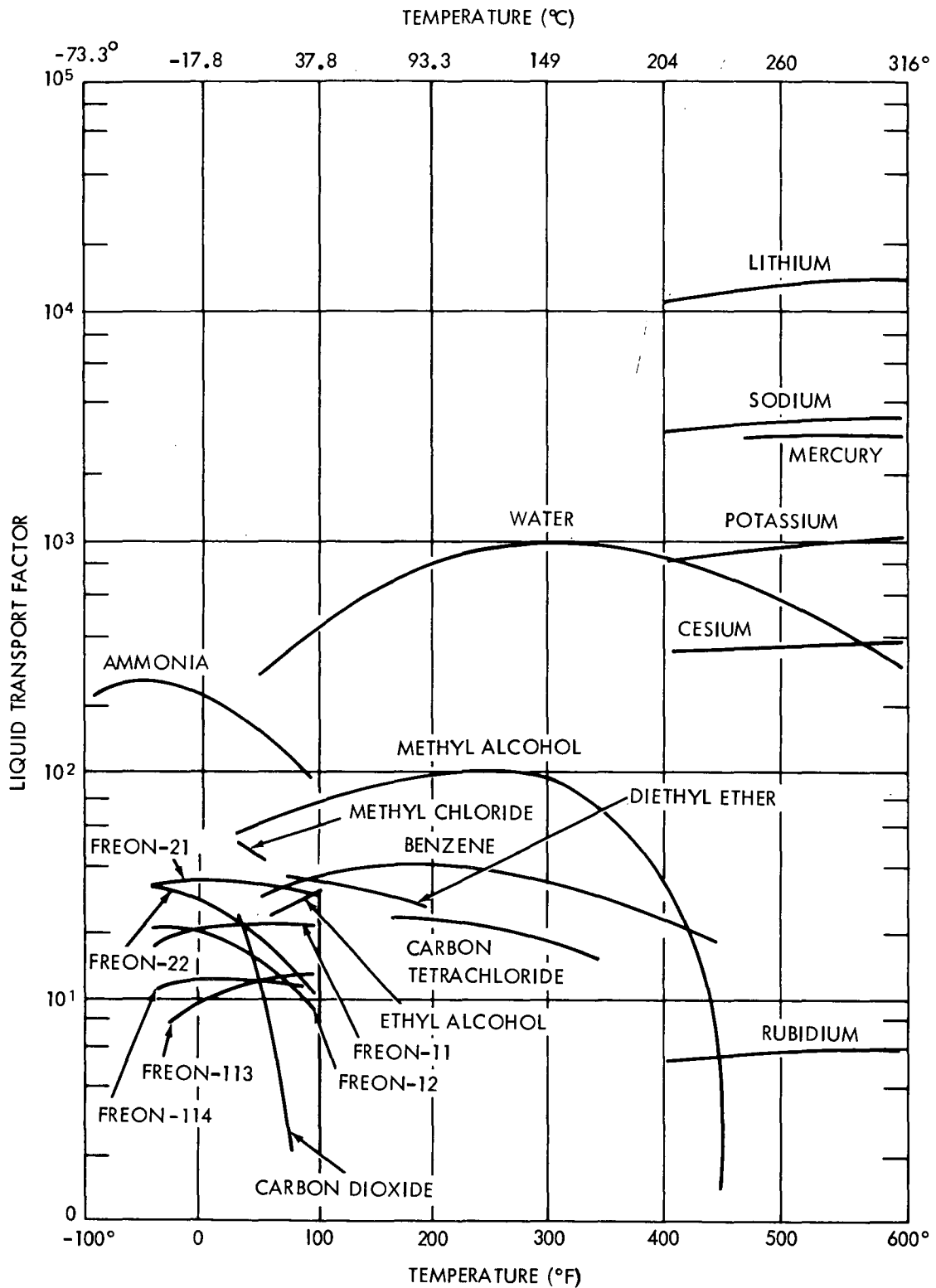


Figure 4. Liquid Transport Factor (Figure of Merit) for Various Liquids

Choice of Container Material

Once the fluid has been selected for a given thermal range, the design of the external container and the selection of the material can be finalized. The criteria which must be considered in selection of the container material are as follows:

1. The fluid and container compatibility;
2. The maximum power density to be absorbed by the pipe; and
3. The external and internal forces acting on the container.

Material. Because the container and the fluid must be chemically compatible, the choice is usually limited to a few pipe materials for any given fluid. The materials which have been used thus far include aluminum, copper, stainless steel, and glass, all tested at Goddard, and nickel, ceramic, and alloys of molybdenum, tantalum, and niobium, which were tested in private industry (Ref. 8).

Aluminum 6061-T6, in the form of a seamless tube, has been the most commonly used material, because of its low weight, ease of machining, and its compatibility with many fluids. Aluminum has been used on heat pipes for the OAO-B, OAO-C, ATS-E, and ATS-F spacecraft.

Other factors involved in the selection of the container material are the machining and heating processes that the item must undergo after it has been charged or filled with its working fluid. These include the types of mechanical support, whether the pipe is bonded or welded in place, and other processes which must be endured while the pipe is being assembled into its final working location.

The problem of processing the tube after filling caused great concern for the ATS-F spacecraft heat pipes, when a high-temperature process became necessary before some of the heat pipes could be completely encased in the protective honeycomb panels which formed the spacecraft walls and support decks. The problems associated with such later processes could require alterations to the diameter and wall thickness of the pipe and to its manufacturing process.

Power Density. The maximum allowable power density, i.e., the maximum heat input into a pipe, is a function of four variables – the input area, the wicking device, the working fluid, and the thermal gradient required by the spacecraft.

Power density specifies watts per unit area, and this is different from total power, since total power can be applied over a large or small area. Thus any given heat pipe system can take only a certain concentration of power before the capillary pumping limit of the wick is overtaxed, and dryout, or burnout, occurs. It is likely that the thermal gradient requirement of any spacecraft which uses heat pipes could be exceeded long before burnout occurs.

The limitation posed by the working fluid is strictly a function of the ability of the fluid to absorb heat via its property, the latent heat of vaporization. Thus much depends upon the fluid which is used; the liquid with the highest h_{fg} will yield a lower thermal gradient for the same power density.

External and Internal Forces. External and internal forces are of prime importance to the proper functioning of the pipe. One of the ammonia-filled pipes for OAO-C had an internal pressure of approximately 200 psig at 20°C. At 54°C, based on the perfect gas law, the pressure was 760 psig. This would have presented a serious health problem to nearby personnel if the pipe had accidentally ruptured or if it had been dropped during testing. The external forces which must be considered are those created by acceleration during launch and by spinning or tumbling in orbit. The pipe must be strong enough to withstand all these forces in combination. Heat pipes with internal pressures of 0.03 to 10 atmospheres have been operated successfully in laboratories for periods of up to 8 years.

Choice of Wicking Device

In addition to the working fluid and the container, the third essential part of the heat pipe is the wicking device, or capillary or wicking structure, which facilitates the movement of the cool liquid to the warm or hot evaporator section of the pipe. As shown by the numerous cross sections of heat pipes in figure 5, the only limit on the basic design of the wicking structure is the experience and imagination of the designer.

The wicking structure is similar to and performs the same function as the wick in a kerosene lamp: it provides a fine-mesh capillary structure which moves the liquid from one point to another, in both cases from a point of high liquid pressure and cooler temperature to a point or points of lower liquid pressure and higher temperature.

The wicking device shown in detail in figure 6 consists of a section of 304 stainless steel screen, 100 mesh per 2.54 cm (1 inch), which is 90.2 cm (35.50 inches) wide and approximately 10.2 m (400 inches) long. This screen is welded along one long edge to a 310 stainless steel wire core 1.6 mm (0.063 inch) in diameter.

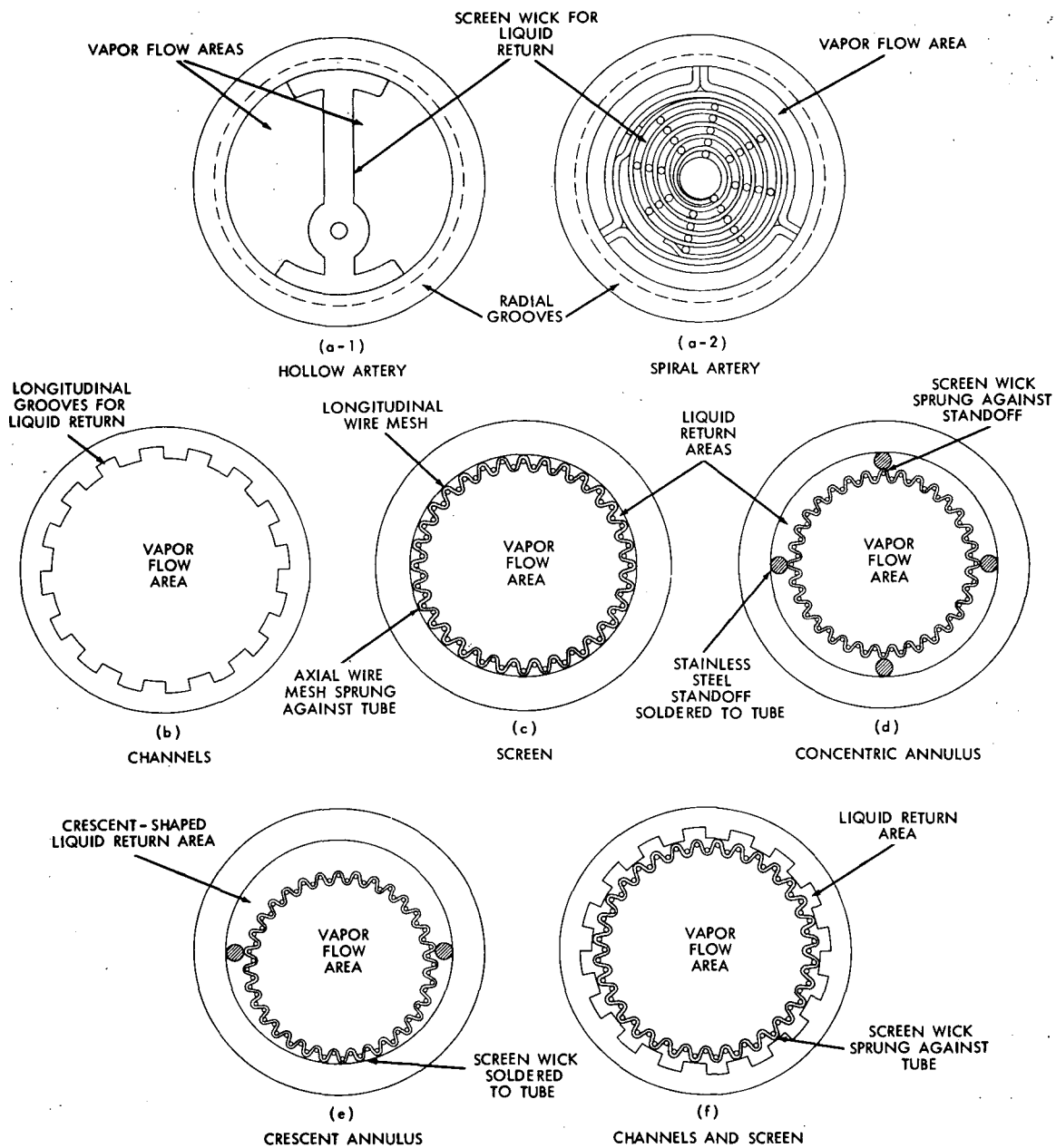


Figure 5. Cross Sections of Various Types of Wicking Devices

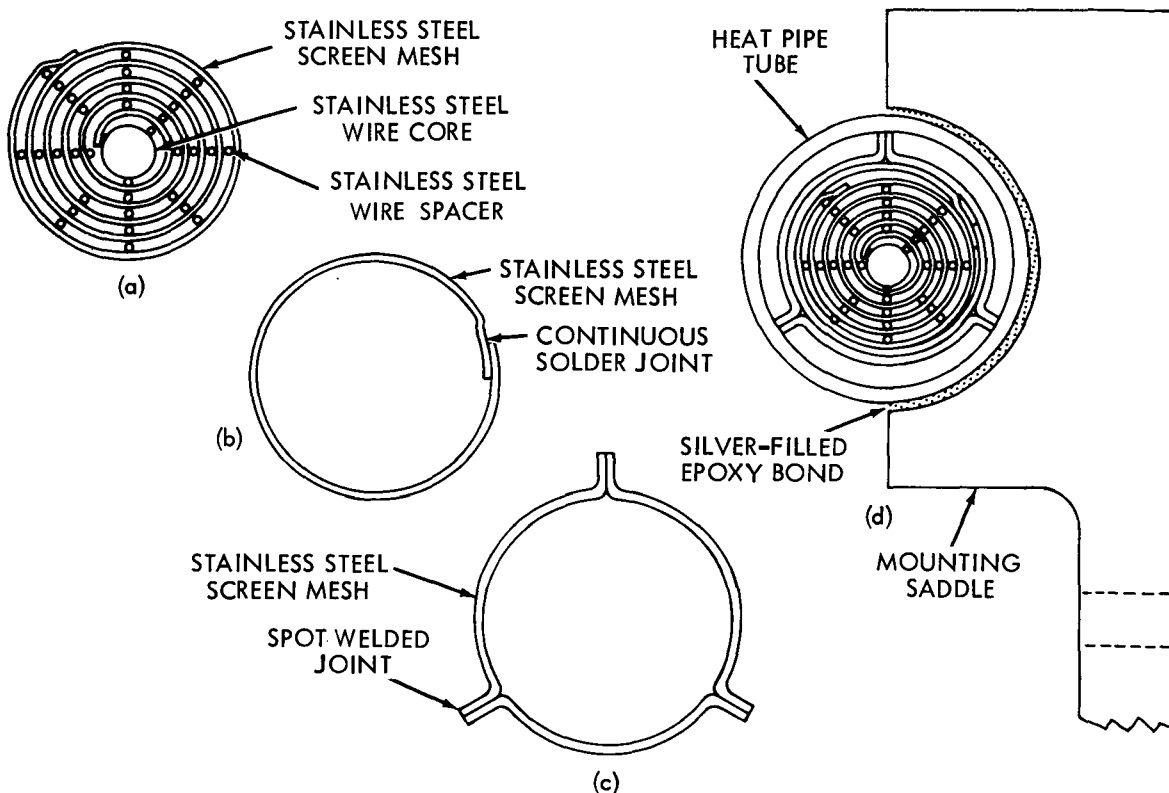


Figure 6. Detailed Views of Artery Wicking Device

Other wires, which serve as spacers, are welded on the mesh at 6.3 mm (1/4-inch) intervals, parallel to the core wire. The whole is then rolled around the core wire (a), figure 6, to form a wick some 3.74 m (147.3 inches) long and 6.5 mm (0.255 inch) in diameter.

This wick is enclosed in a cover or sock (b), also formed of the stainless steel 100 mesh; and this in turn is surrounded by the artery retainer (c), made of the same mesh screen, which supports the wick and makes contact with the outside wall. The entire wick is then forced into the heat pipe tube (d), and the whole is rounded into the shape of a torus of 1.19-m (46.9-inch) diameter, with a nominal 10-cm (4-inch) gap.

There are many reasons for the wicking structure. In addition to helping the return flow of cool liquid to the hot sections of the pipe, the wicking structure provides for better wetting of the entire interior structure. The wicking structure provides the major driving force for the heat pipe, because of the pressure forces which exist across each meniscus, the curved upper surface of a column of liquid, pressure forces which would not exist without the wick. The wicking structure is used in most heat pipes, the notable exception being a rotating, tapered pipe (figure 7) which utilizes inertial forces to distribute the

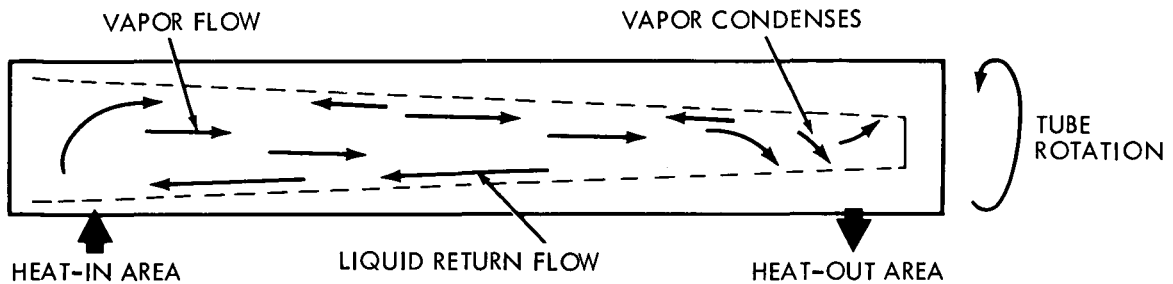


Figure 7. Wickless Heat Pipe

working fluid. When used in a 1-G field the rotating type is actually a reflux boiler, in which the liquid flows back to be heated again, and it is not a heat pipe if the heat-in area is lower than the heat-out area.

The mesh screen is commonly used in wicking structures, in both the homogeneous and nonhomogeneous types. The homogeneous type has one type of mesh material and one pore size throughout. The nonhomogeneous type may have different mesh materials or different pore sizes in various parts of the pipe, or the wicking structure may have two layers, with a coarse wire mesh next to the pipe walls, to permit the easier flow of the liquid along the pipe walls, and a fine wire mesh on the inside, next to the vapor flow passage, where it produces a large capacity in capillary pumping. Fine mesh increases the capillary pumping capacity, but it also increases the frictional resistance to the movement of the liquid.

Extensive work at the Los Alamos Laboratories (Refs. 9, 10, 11) indicate that artery-type returns, with the wicking structure, are necessary in the longer heat pipes, and that the nonhomogeneous wicks are better than the homogeneous type.

For fluids other than liquid metals, which were not included in this investigation, good thermal contact between the wicking structure and the walls of the tube is essential for efficient heat transfer and for the minimization of the radial temperature gradients ΔT (Ref. 11). The reason is obvious: the better the contact the lower the thermal resistance. When operating in a zero-G field a wicking structure of any diameter will fill readily and will coat the walls if

enough liquid is available to saturate the wick. This is not the case in a 1-G field, where the gravitational pull prevents the higher portions of the wick from filling as rapidly and completely as the bottom portions of the wick. However, ethyl alcohol in a small diameter (3 mm) tube is an exception; this liquid has extremely good wettability characteristics (Ref. 12). The degree to which other liquids can fill and coat the walls of larger diameter tubes is given (Ref. 13) as a function of

$$\sqrt{\frac{\sigma}{\rho_l}}$$

This states that the greater the surface tension and the lower the liquid density, the easier it is for a liquid to expand throughout a wicking structure.

Method of Charging a Heat Pipe

Charging a heat pipe with a working fluid is a difficult task because of the necessity of having a clean pipe and a pure, uncontaminated fluid. Extreme care must also be taken to ensure that all foreign matter is removed from the pipe prior to charging to prevent a possible chemical reaction which could lead to the generation of a noncondensable gas or to the formation of sludge.

Normally the heat pipe container is cleaned many times, baked out, and evacuated with a vacuum pump. After this a supply of the working fluid is connected via a vacuum system to the evacuated pipe, and the fluid is slowly leaked into the system until the desired weight of fluid has entered the pipe. Once this occurs the line connecting the heat pipe to the vacuum system is pinched off about one-half inch from the pipe and is sealed. The major danger during any of these steps is the inclusion of gases other than the gas and fluid desired.

HEAT PIPE OPERATION

The heat pipe operation can be described simply, with reference to figure 8, as follows: The fluid-vapor combination creates a closed, flowing system. Prior to the application of heat, the fluid is in a steady-state, no-flow condition. As heat is introduced in the evaporator section, the local liquid is vaporized, causing a local increase in vapor pressure, which results in a vapor pressure differential along the pipe. This vapor pressure gradient provides the driving force which causes the vapor to flow into the colder or condenser section of the pipe.

Once the hot vapor reaches the colder sections of the pipe, condensation occurs, and the liquid returns to the evaporator section via capillary action through the wicking structure or artery. As soon as the vapor begins to condense a liquid-pressure gradient is created, which may, under the influence of gravity, aid the return of the fluid to the hot sections. Since there is virtually no gravitational effect in orbit, this gravitational force is counteracted during testing by placing the heat pipe on the tilt-table, and providing a slightly uphill path for the liquid return. This also avoids the hydrodynamic head or pressure formed by puddling of the liquid, which could aid the return flow of fluid to the evaporator.

The dominant driving force for the liquid return, the capillary action of the wicking structure, is a result of the fluid surface tension. Even in a 1-G environment and in contact with a solid object, the liquid tends to create minimum surface shapes. These shapes are distorted, however, because of the adhesive forces which exist between unlike substances.

In a heat pipe with sufficient liquid the wick will draw continuously upon the available liquid, in order to continuously recreate minimum surface shapes; this is the mechanism and motion called capillary action. This capillary action is always toward the hotter and drier sections. The net result of this capillary action is fluid flow, and under the proper conditions this flow can be rapid.

In a nondynamic, zero-G condition, pipe flow as a result of capillary action will continue indefinitely. As mentioned previously, the flow of the fluid in a vertical direction in a 1-G field will stop once the weight of the liquid column being supported equals the force of gravity acting against it.

In examining the modes of heat transfer, it is noted that three modes can occur: surface evaporation, nucleate boiling, and film boiling, which is a special case of nucleate boiling. Conduction of heat through the liquids and vapors is

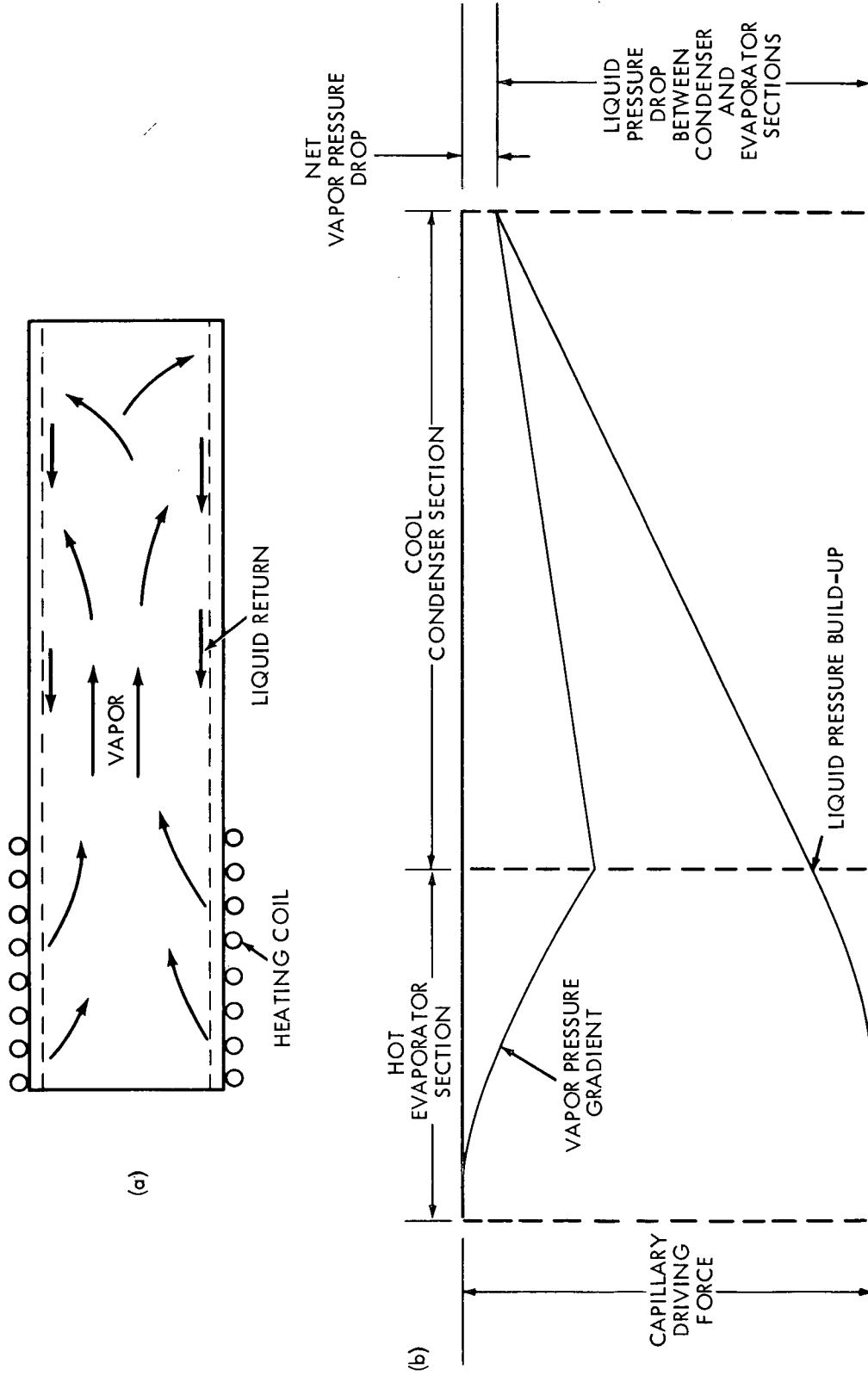


Figure 8. Heat Pipe Circulation and Pressure Diagrams

small, compared with metals. Under controlled conditions the evaporation of the fluid in heat pipes is accomplished by surface evaporation, which as the name implies is the evaporation of molecules at the liquid-vapor interface. Nucleate boiling is the formation of vapor bubbles around small particles which serve as nuclei. There is strong experimental evidence (Ref. 14) that this type of boiling can be avoided by using ultraclean fluids in ultraclean pipes.

Film boiling is the condition where a film forms on the surface being heated, such as the bottom of a pan. As the heat input continues or increases, the film layer thickens until its buoyancy force exceeds the surface tension force, causing the film to break away and to rise to the surface of the liquid. Film boiling will not occur in a heat pipe unless local heat inputs create an overdriven condition, causing rapid dryout in the pipe (Ref. 15). Dryout is a failure of the system to function, and is to be avoided in all operational cases. As in the case of steam boilers, the design of the heat pipe must be such that film boiling is negated, or large thermal gradients will occur, resulting in dryout of the heat pipe.

Because evaporation and condensation may occur anywhere along the length of the tube, and are basically independent functions, the heat pipe tends to be a self-regulating and isothermal system (Refs. 5, 16, 17). Radial gradients, however, can exist. This is because the cross-sectional areas of the pipes vary, due to the porous wicks, causing non-uniform flow patterns. Further, non-uniform contact of the wick with the shell creates additional radial gradients. These gradients can be of the order of several degrees. Since this is basically an internal problem and cannot be measured with techniques available to date, only the longitudinal gradient is seen and is measurable.

GOVERNING ANALYTICAL EQUATIONS

Pressure Gradient Equations

As indicated above, a heat pipe consists of a sealed tube, a working fluid, and a wicking structure. The wick volume contains the liquid phase of the working fluid, and the remaining volume of the pipe contains the vapor phase. In operation, heat is applied to one section and is removed from another, establishing a two-phase, counter-current flow regime. Evaporation and condensation can occur at any place in the pipe where the liquid-vapor interface exists.

The heat input and removal cycle, as mentioned previously, consists of five steps: (1) vaporization of the local liquid in the heat input area; (2) movement of the hot vapor to the cooler section of the pipe; (3) conduction of the heat through the container wall; (4) condensation of the vapor into a liquid; and (5) return of the liquid through the wick to the warm area by capillary attraction.

Fluid circulation in the pipe is thus maintained by the capillary forces which develop in the wick structure at the liquid-vapor interface. For steady operation (see Figure 9) this flow can be expressed in pressure terms as follows:

$$P_{fe} = P_{ge} - (P_{ge} - P_{gc}) - (P_{fc} - P_{fe}) - \text{Gravity forces} \quad (1)$$

OR

$$P_{ge} - P_{fe} = (P_{ge} - P_{gc}) + (P_{fc} - P_{fe}) + \text{Gravity forces} \quad (2)$$

OR

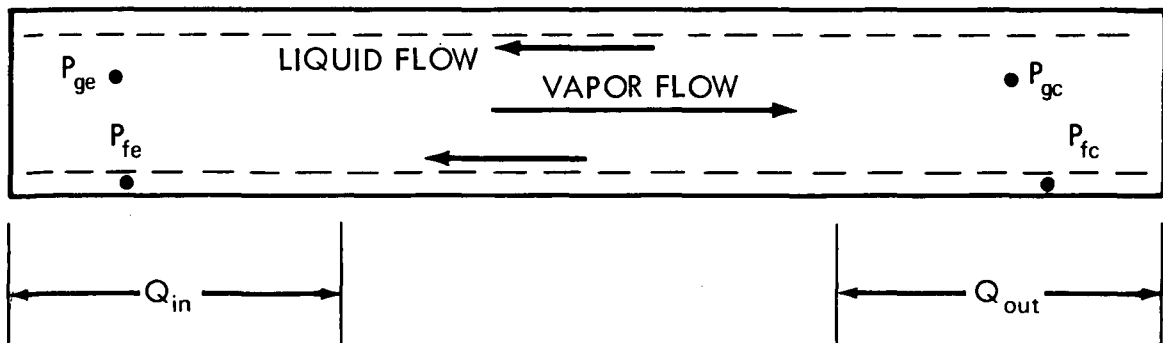


Figure 9. Heat Pipe Steady Operation Pressure Terms

Preceding page blank

$$\Delta P_c \geq \Delta P_g + \Delta P_f + \Delta P_s \quad (3)$$

where

ΔP_c = Capillary pumping pressure,

ΔP_g = Vapor flow pressure drop,

ΔP_f = Liquid flow pressure drop,

ΔP_s = Gravitational force,

P_{fe} = Pressure of the fluid in the evaporator,

P_{ge} = Pressure of the gas in the evaporator,

P_{gc} = Pressure of the gas in the condenser, and

P_{fc} = Pressure of the fluid in the condenser.

Equation (3) expresses the necessary capillary pull required for the heat pipe to function. While this equation looks simple, the determination of each quantity is very difficult. A discussion of each of these terms follows.

Capillary Pumping Pressure

The capillary forces have to balance the pressure losses due both to vapor and liquid drag and to the gravitational differences when in a 1-G environment. This is accomplished by many tiny menisci, for a screen wick, that form at the vapor-liquid interface. This allows the vapor pressure to be higher than the liquid pressure throughout the heat pipe. For a screen or channel system, a typical meniscus is characterized by two principal radii (r_1 , r_2) of curvature. Thus at any point, the pressure drop across the liquid-vapor interface is given by

$$\Delta P_c = \sigma \left(\frac{1}{r_1} + \frac{1}{r_2} \right) \cos \theta. \quad (4)$$

If the working fluid wets the wick completely, $\theta = 0$ degree, this equation yields the maximum capillary force (ΔP_c). This is because once the heat transfer limit is reached, the liquid meniscus will be defined exactly by the wicking structure being used. However, for longitudinal channels the radius of curvature

along the major axis of the channel can and does become very large, and, therefore, this radius of curvature is ineffective in determining ΔP_c . Thus only the circumferential radius across the channel is important. For steady-state operations this radius is smallest in the evaporator, because of fluid evaporation, and will decrease with increased heat loads until it approximates half the channel width. When this occurs the limiting heat transfer case has been achieved, and ΔP_c can be expressed as:

$$\Delta P_c = \frac{\sigma}{r}, \quad (5)$$

where $r = 1/2$ the channel width and $\theta = 0$ degree. If $\theta \neq 0$ degree, $r = r_1 \sec \theta$, where $r_1 =$ liquid radius of curvature. Therefore, by equating r_1 and r_2 in equation (4), it is proven that ΔP_c max for screens is double that for grooves of the same mesh size.

Liquid Pressure Gradient

Equations to express the liquid-pressure drop along the pipe are much more complex than those used to express ΔP_c . Some simplifying assumptions can be made. The most useful of these assumptions is that the radial pressure differences are much less than the axial-length pressure gradients. This in general is a valid assumption, because the axial length of the pipe, L , is much greater than its radius, r_p . Poiseuille's equation is useful for expressing the liquid pressure drop through a capillary tube. This is given as

$$\Delta P_\ell = \frac{8 \mu_\ell \dot{m}_\ell L}{\pi r^4 \rho_\ell}, \quad (6)$$

where

μ_ℓ = liquid viscosity,

\dot{m}_ℓ = liquid mass flow rate,

L = tube length,

ρ_ℓ = liquid density, and

r = tube radius.

Equation (6) can be re-expressed for the cross-sections of the pipes shown in figure 5 as follows (see Ref. 18):

$$(a) \text{ Artery} \quad \Delta P_\ell = \frac{8 \mu_\ell Q L_e}{\pi r^4 \rho_\ell h_{fg}} \quad (7)$$

$$(b) \text{ Channels} \quad \Delta P_\ell = \frac{8 \mu_\ell Q L_e}{\pi r_e^4 N \rho_\ell h_{fg}} \quad (8)$$

$$(c) \text{ Screen} \quad \Delta P_\ell = \frac{b \mu_\ell Q L_e}{\pi (R_w^2 - R^2) \epsilon r_c^2 \rho_\ell h_{fg}} \quad (9)$$

$$(d) \text{ Concentric Annulus} \quad \Delta P_\ell = \frac{12 \mu_\ell Q L_e}{\pi D W^3 \rho_\ell h_{fg}} \quad (10)$$

$$(e) \text{ Crescent Annulus} \quad \Delta P_\ell = \frac{4.8 \mu_\ell Q L_e}{\pi D W_e^3 \rho_\ell h_{fg}} \quad (11)$$

where

- L_e = effective heat pipe length,
- r_e = effective channel radius,
- N = number of channels,
- b = screen tortuosity factor,
- R_w = outer radius of screen,
- R = vapor flow passage radius,
- ϵ = screen void fraction,
- r_c = effective radius of screen openings,
- D = mean diameter of annulus,
- W = width of annulus,
- Q = rate of heat transfer from one section to another section of the heat pipe,
- h_{fg} = latent heat of vaporization, and
- W_e = effective width of annulus.

Vapor Pressure Gradient

Vapor flow in the evaporator and condenser sections of the pipe is dynamically identical to pipe flow with injection or suction through a porous wall, and is a function of the Reynolds number. If the Reynolds number is $\ll 1$, viscous effects dominate the inertial effects of the flow, and formula (6) can be used to determine the vapor pressure drop along the pipe (Ref. 19).

$$\frac{dP_f}{dL} = \frac{-8 \mu_v \dot{m}_v}{\pi \rho_v r_v^4} \left(1 + \frac{3}{4} R_e - \frac{11}{27} R_e^2 + \dots \right), \quad (12)$$

where:

μ_v = vapor viscosity,

\dot{m}_v = vapor mass flow rate,

ρ_v = vapor density

r_v = vapor flow radius, and

R_e = Reynolds number.

The negative sign is used since the pressure decreases along the flow path.

Equation (12) is the result of assuming a Poiseuille flow pattern with an expanded perturbation expression used for the velocity. This is used because it is known that in the evaporator and condenser sections of the heat pipe the velocity profile departs from that of Poiseuille flow.

When evaporation rates are high ($R_e \gg 1$ but < 2000) and the flow becomes boundary layer flow, the pressure begins a dynamic recovery in the condenser sections. For this case, the following equation is used (Ref. 9):

$$\frac{dP_f}{dL} = \frac{-S \dot{m}_v}{4 \rho_v r_v^4} \left(\frac{d \dot{m}_v}{dL} \right), \quad (13)$$

where

$$S = 1 \text{ for the evaporator sections and } 4/\pi^2$$

for the condenser sections.

If fully turbulent flow develops, the empirical Blasius equation can be used to express ΔP_v . This is given by:

$$\frac{d P_f}{d L} = \frac{-0.0655 \mu_v^2 R_e^{7/4}}{\rho_v r_v^3} \quad (14)$$

This equation should be used when $R_e > 2000$ (Ref. 20).

Thus a major gap exists between the flow regions covered by equations (12) and (13); that is, the case for $R_e = 1$ is not covered. Further, since the velocities are extremely difficult to measure the R_e cannot be accurately determined, and the appropriate equation to be used is questionable. The Reynolds number is given as:

$$R_e = \frac{\rho_l D V}{\mu_l} \text{ which can be re-expressed as}$$

$$R_e = \frac{\dot{m}_v}{\pi r_v \mu_v}$$

where

D = pipe diameter,

V = average velocity across
the vapor flow passage.

Thus we are stranded analytically with three equations. However, pipe flow experiments other than those with heat pipes have enabled the determination of the onset of turbulence as a well defined function of the Reynolds number. These results are: If $R_e > 1000$ and $L > 50 r_p$ use equation (13); if $R_e > 2000$, use equation (14).

An extension of these analyses to include a method to determine ΔP_c from simpler tests, expressions for the mass flow rates, boundary conditions, and heat transfer equations follows.

Equations of Motion, Continuity, and Heat Transfer with Boundary Conditions and Flow Limitations

In any convective heat transfer situation, a minimum of three equations are necessary to describe the problem. These are (1) the equation of motion, (2) the continuity equation, and (3) the governing heat transfer equation. With a complete set of boundary conditions, an analytical solution can be achieved if the governing equations are of sufficient simplicity. For heat pipe analysis and understanding, the equations of motion are given along with the hydrostatic equation, since gravity effects in a 1-G field can be great in the first case and the only factor in the latter. Velocity boundary conditions are presented, mass flow rate equations, thermal gradients equations, and a list of flow inhibitions and limits are also included to aid in a more complete understanding of the situation.

Equation of Motion. The equation of motion is actually three equations, but can be written in vector form as:

$$\frac{D \vec{v}}{D t} = -\frac{\nabla p}{\rho} + \mu \nabla^2 \vec{v} + \vec{g} \quad (15)$$

where $D () / D t$ is the substantial or material derivative, which is expressed as:

$$\frac{\partial ()}{\partial t} + \frac{u \partial ()}{\partial x} + \frac{v \partial ()}{\partial y} + \frac{w \partial ()}{\partial z} .$$

The hydrostatic equation is evolved when $v = 0$:

$$\nabla p = \rho \vec{g} . \quad (16)$$

If we assume \vec{g} acts only in the vertical direction; i.e., $\vec{g} = g_0 \hat{h}$, equation (15) becomes

$$\nabla p = h \rho g \sin \phi = \Delta P_g \quad (17)$$

where

ϕ = pipe tilt angle departing from a horizontal position.

ΔP can also be expressed as the difference in static pressure due to the weight of liquid between two sections in the pipe. Gravitational effects are assumed zero for the vapor flow sections, and for analytical purposes the gas is assumed to have a Boltzmann distribution in a 1-G field. The pressure difference would be a maximum between the two pipe ends. Since the gravitational effects can be evaluated rather easily, a simple method to determine ΔP_c in a static condition can be achieved.

Analytical Determination of ΔP_c . Figure 10 shows a typical liquid profile supported by the wicking structure of the heat pipe. As noted, the liquid profile is not necessarily uniform. However, across each of the local liquid-vapor interfaces a pressure balance exists. This can be shown to be equal to:

$$P_v(L) - P_l(L) = \frac{2\sigma}{r(L)}. \quad (18)$$

Equation (18) is a function of position as noted. Now, in a static state, all pressure differences are equal. Thus equating equations (17) and (18) and solving for h yields

$$h_{\max} = \frac{2\sigma \cos \theta}{\rho_l g r_c \sin \phi}, \quad (19)$$

where

$$r(L) = r_c(L) / \cos \theta.$$

Equation (19) provides an analytical expression which can be used to predict ΔP_c . (Note: $\Delta P_c = \rho g h_{\max}$.) This can be checked experimentally under static conditions by the diagram shown in figure 2. For a steady state operating pipe, r_c varies along the pipe. If θ is assumed to be zero degree, the only problem in solving equation (19) comes about in the value used for r_c . This radius, r_c , a variable, is minimized in the hot sections of the pipe as the liquid is depleted. Thus, r_c approaches 1/2 pore diameter of the wire mesh in the evaporator sections of the heat pipe as the maximum heat transfer rate is approached.

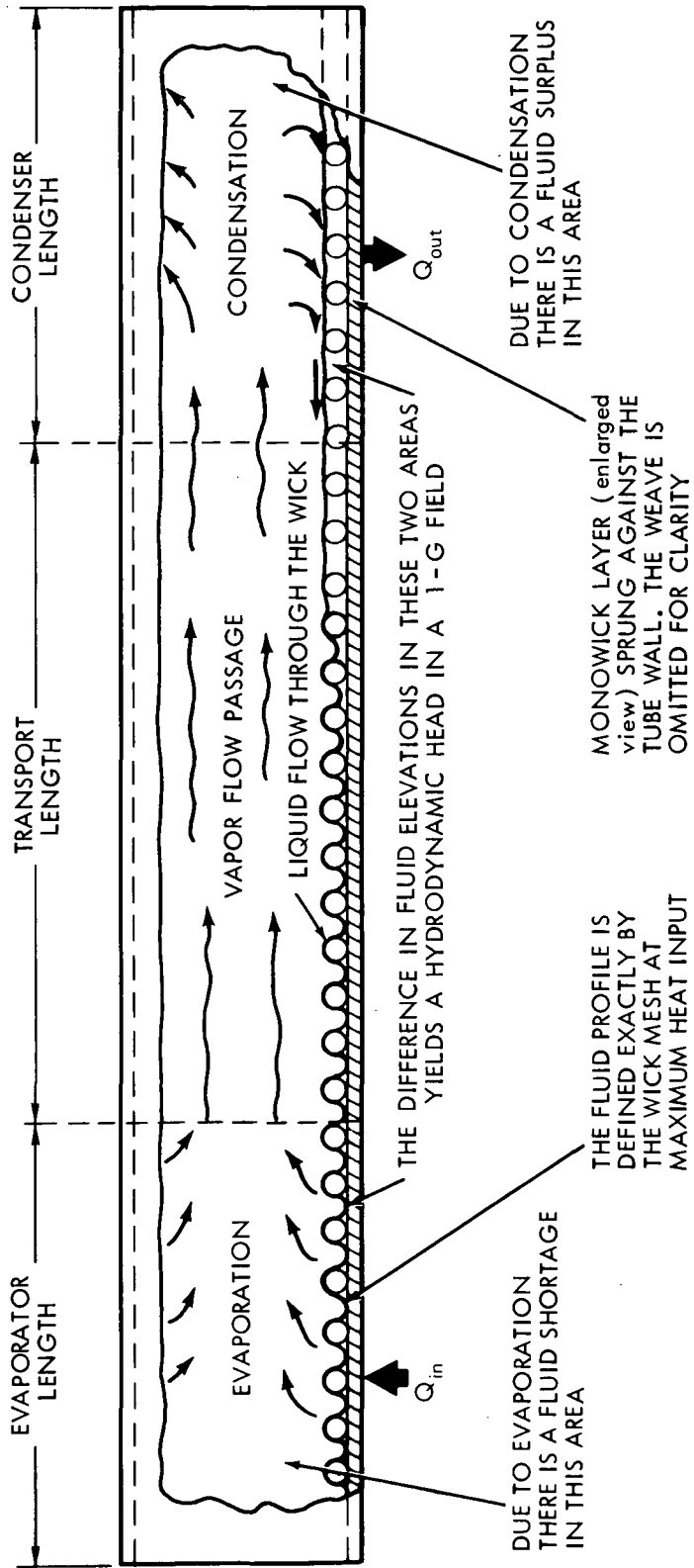


Figure 10. Heat Pipe Vapor-Liquid Interface

In the cold sections of the pipe the radius of curvature, r_c , approaches infinity due to excessive fluid buildup of condensed fluid.

Boundary Conditions and Mass Flow Rates. The conservation of mass equation can be expressed in vector-form as:

$$\nabla \cdot \rho \vec{V} = 0 \quad (20)$$

where

$$V = V(L, r_w) = V(0, r) = V(L, r) = 0.$$

In other words, the velocity at the walls and at the tube ends is zero. (See figure 11.) Now assuming that the vapor density is given as $\rho_v(L, r)$, and that the velocity is given as $v_v(L, r)$, the vapor mass flow rate can be expressed as:

$$\dot{m}_v(L) = \int_0^{r_v} \rho_v(L, r) V_v(L, r) 2\pi r dr \quad (21)$$

where

r_w = wall or wick radius, and

r_v = vapor flow passage radius.

Likewise an expression for the mass flow rate in the liquid phase can be expressed as:

$$\dot{m}_\ell(L) = \int_{r_v}^{r_w} \rho_\ell(L, r) V_\ell(L, r) 2\pi r dr, \quad (22)$$

and based on the conservation of mass principle:

$$\dot{m}_\ell(L) + \dot{m}_v(L) = 0. \quad (23)$$

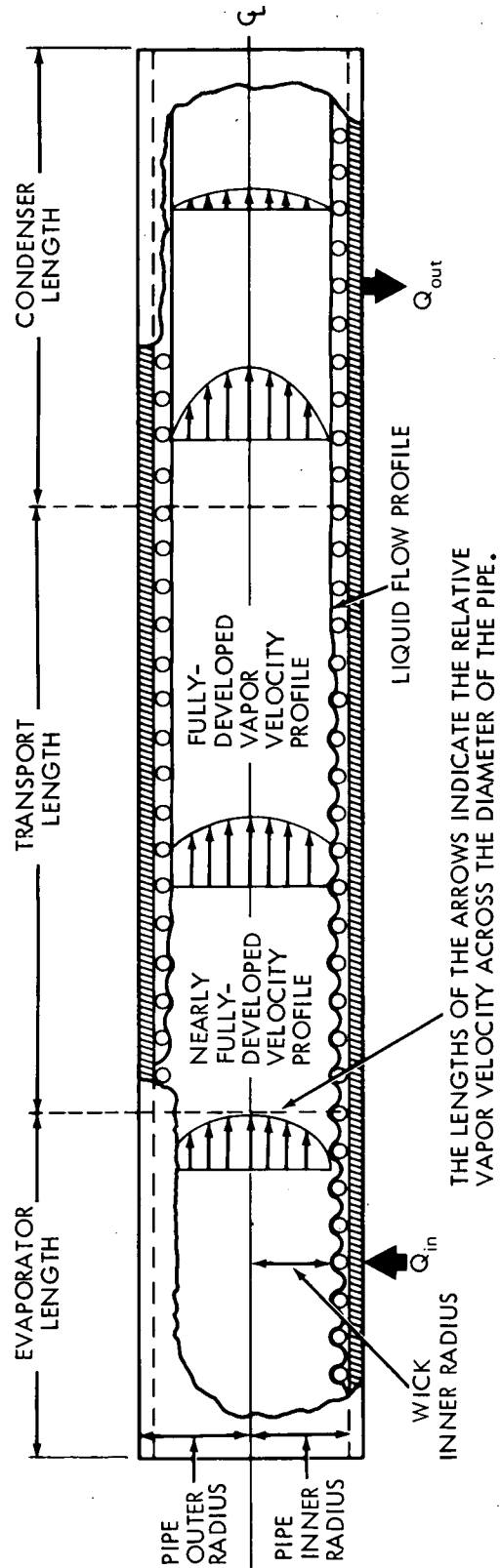


Figure 11. Vapor Velocity Profile within a Heat Pipe

Therefore, once either of the mass flow rates has been determined the other is also determined.

Heat Transfer. For the steady-state transportation of heat, the energy equation can be written in vector-forms as:

$$\nabla \cdot \vec{Q} = 0, \quad (24)$$

where

$$\vec{Q} = h \rho \vec{V} - \vec{k} \nabla T. \quad (25)$$

By definition, the heat pipe functions when the axial and radial thermal gradients are small, even though the heat transport may be large (Ref. 9). Axial conduction is neglected since the heat pipe has small wall thickness. Therefore:

$$Q = \int_0^{r_v} h_v \rho_v V_v 2 \pi r dr + \int_{r_v}^{r_w} h_\ell \rho_\ell v_\ell 2 \pi r dr. \quad (26)$$

Substituting for the mass flow rates yields:

$$Q = h_{fg} \dot{m}_\ell (L). \quad (27)$$

Thus it is seen that the axial transport of heat is maximum at the end of the evaporator, and can be expressed as the product of the latent heat of vaporization times the mass flow rate.

Thermal Gradients. A simple relationship that aids in theoretically determining the vapor temperature from the pipe temperature is given by:

$$T_p = T_v + H_T/K, \quad (28)$$

where

H_T = heat added per unit length in the evaporator, and

$$\frac{1}{K} = \frac{1}{2\pi} \left[\frac{1}{K_p} \ln \left(\frac{r_p}{r_w} \right) + \frac{1}{K_w} \ln \left(\frac{r_w}{r_v} \right) \right] \quad (29)$$

where

- r_p = pipe radius,
- K_p = thermal conductivity of the pipe, and
- K_w = thermal conductivity of the wick.

The temperature drops in the vapor section of the heat pipe can be obtained by using the Clapeyron-Clausius equation:

$$\Delta T_v = T_v(L) - T_v(0) = \frac{R T_0^2 \Delta P}{M h_{fg} P(T_0)}, \quad (30)$$

where ΔP is small. This equation is good when the pipe is completely wet, has small thermal gradients, and utilizes nothing but surface evaporation to complete the change of state from liquid to vapor.

Flow Limitations: Entrainment. If a heat pipe is functioning properly, its maximum heat-carrying capacity can be achieved. This occurs when the flow is stable, the wick is completely wet, no hot spots exist, and small pressure gradients serve as the driving forces for liquid and saturated vapor flows.

Any slight departure or perturbation of this balanced flow condition by excessive heating rates could cause liquid drops to form in the vapor flow passage and could lead to a condensation shock. If a shock should occur, two-phase flow in the vapor channel would result. To lessen the possibility of two-phase flow in the vapor passage, it is essential to limit large areas of liquid surface from high vapor-velocity flow regions. Thus if capillary grooves are aligned in the flow direction, such as the OAO-B and ATS-F grooved pipes, and are unprotected, a thermal limit due to condensation shock could occur (Ref. 21).

The entrainment of liquid drops into the vapor flow passage is due to dynamic instability at the liquid vapor interface. According to linear theory (Ref. 22), a given vapor of density ρ_v , flowing at a velocity of V_v past a nearly stationary liquid with surface tension (σ), will create a small amplitude wave which departs from the normal surface with wave-length λ and will grow exponentially with time if

$$\frac{\rho_v V_v^2 \lambda}{2\pi\sigma} > 1. \quad (31)$$

Equation (31) is the ratio of dynamic forces to surface tension forces, and is called the Weber number. This equation is a measure of the capture of liquid drops in the vapor flow passage from wave crests caused by the perturbed conditions. This condition, if achieved, will cause the heat pipe to stall and the evaporator to overheat. Experimentation to date has shown that the use of fine mesh wire wicks tends to prevent liquid capture.

Other Heat Flow Limitations. Other limitations are (1) overheating (local hot spots) in the evaporator sections due to lack of sufficient liquid return; (2) insufficient return of liquid as limited by the capillary pumping mechanism; (3) limits due to counter current shear at the liquid-vapor interface; and (4) sonic limit, choke flow.

TEST CONFIGURATION

Based upon knowledge of how heat pipes work, analysis of test data can be interpreted to yield intricate details of functionality. To obtain these details, it is essential to have a flexible test setup.

As shown in figure 12, the test configuration for each of the high-power heat pipes included a mobile tilt table, on which the individual pipes were mounted on teflon standoffs, with two flight heaters, four test heaters, and numerous thermocouples to monitor the temperature. In the center foreground is shown the vacuum-rated motor, used to change the relative elevations of the evaporator

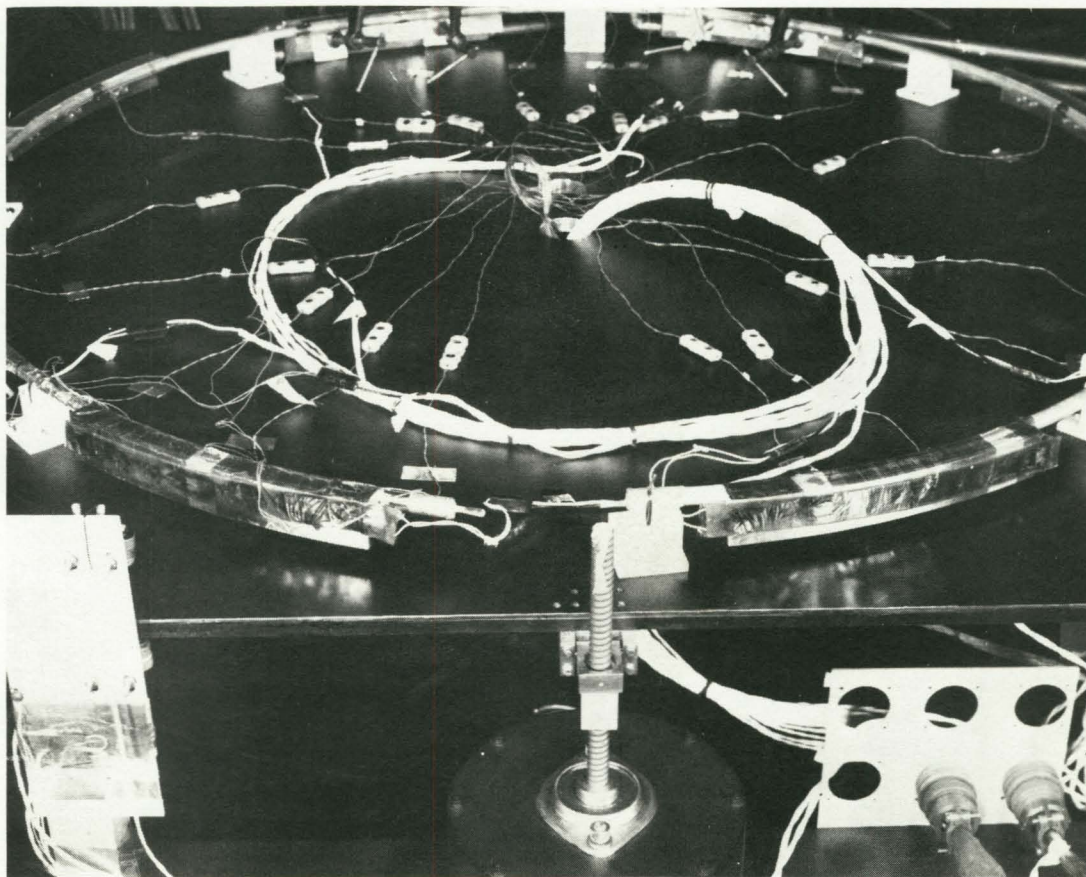


Figure 12. Test Configuration: Heat Pipe Mounted on Tilt Table

and condenser sections of the heat pipe, with a 3.8-cm (1-1/2-inch) tilt available. Also shown in the foreground are two of the test heaters, attached to two of the heat-pipe mounting saddles and wrapped with insulation. The lines from the thermocouples were run through a central hole in the table top to recorders.

The table with the mounted heat pipe and equipment was then pushed into the thermal-vacuum chamber, as shown in figure 13, for the tests. At the left rear of the vacuum chamber may be seen the pipes from the Conrad cooling unit, used to lower the temperature of one or both condenser sections of the tube. This heat-removal system operates between -65°C and $+50^{\circ}\text{C}$ with a controllable accuracy of $\pm 2^{\circ}\text{C}$. The chamber was established at a vacuum of approximately 10^{-7} torr, and the cold walls were controlled from -40°C to $+20^{\circ}\text{C}$.

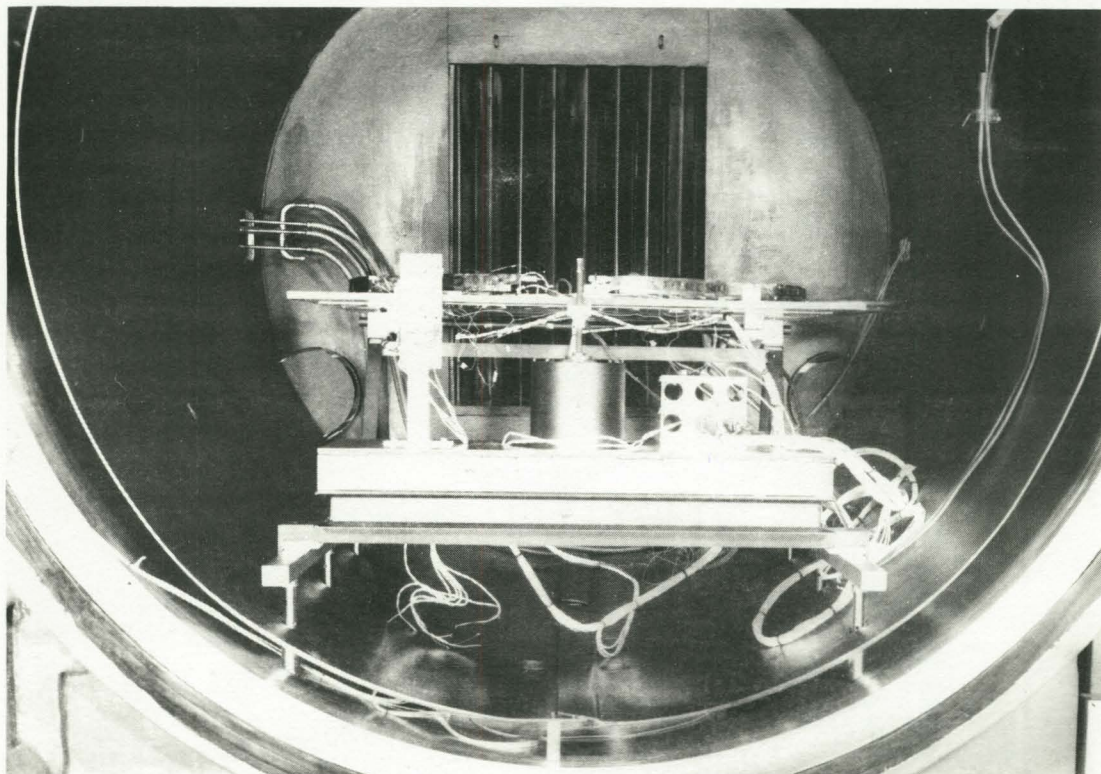


Figure 13. Thermal-vacuum Chamber Setup

The locations of the test and flight saddle heaters and of the 18 thermocouples are shown in figure 14. The thermocouples were placed to monitor the heat pipe temperatures and also the operation of the heaters and of the Conrad cooling lines to the condensers. Power levels for the test heaters could be varied from 0 to 100 watts, for flight heater No. 1, from 0 to 50 watts, and for flight heater No. 2, from 0 to 25 watts. Cross sections of the heat pipes tested are shown in figure 5 (a-1) and (a-2) and in figure 6.

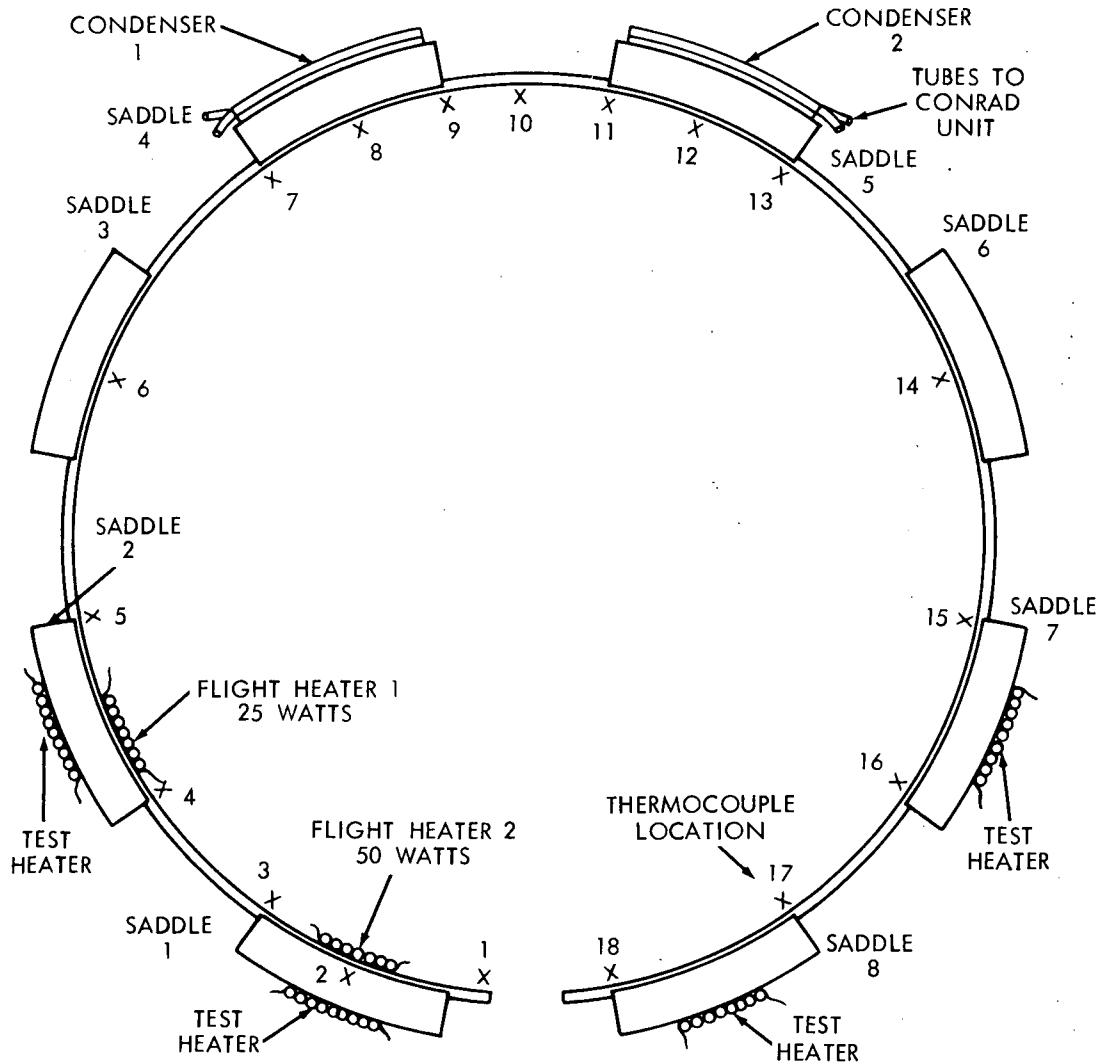


Figure 14. Locations of Heaters, Condensers, and Thermocouples

TEST RESULTS AND CONSIDERATIONS

Performance Requirements

Heat pipes have a good future if they are designed and constructed with extreme care. Mathematical models exist today, but nothing works perfectly all the time, and thus thermal-vacuum and bench testing become essential. Since most pipes will be required to operate for 12,000 to 20,000 hours and longer, under the conditions of vacuum and large temperature extremes, it is essential that rigorous testing for performance and material compatibility be conducted (Ref. 23).

The generation of even a small amount of hydrogen gas in an ammonia or freon heat pipe can create a binary-gas situation which results in poor pipe performance. This is a direct result of the light hydrogen gas being swept down the pipe by vapor-pressure differences. Once in the condenser sections of the pipe, the hydrogen gas blocks a portion of the condenser, and prevents condensation of the working fluid along the condenser. If the heat pipe is blocked the evaporator sections become warmer and the condenser sections become colder, resulting in large gradients which defeat the purpose of the heat pipe. A tiny quantity of water vapor, as little as 50 parts per million, can completely ruin the functioning of a heat pipe. The inclusion of hydrogen gas was shown recently to be the cause of the failure of an OAO-C heat pipe while it was undergoing a thermal-vacuum test (Ref. 24).

The water vapor probably entered the pipe while the pipe was being sealed. The problem was corrected by emptying, cleaning, and carefully recharging the tube. The retesting of this pipe, which will be flown on the OAO-C spacecraft, was successful (Refs. 25, 26). Hydrogen gas problems also occurred with the ATS-F internally-grooved pipes. In that instance the source of the hydrogen gas was not determined, but it might have been generated by a reaction between the ammonia and a solvent residue left in the pipe. These difficulties with hydrogen gas indicate that while heat pipes have the ability to isothermalize the structure they surround, their functioning is very sensitive to cleanliness, to the purity of the working fluid, and to the fluid-container compatibility.

Basic Test Philosophy and Goals

The OAO-C heat pipes were tested under thermal-vacuum conditions to provide a means of evaluating two performance requirements: (1) the degree of isothermalization required under all test conditions, and (2) the high-heat transport

capability, which greatly exceeds the requirements of the mission. Necessary conditions for high performance are that the fluid must prime the artery and that bubbles formed in the artery must readily dissolve.

A considerable amount of data and experience were obtained in testing the OAO-C spacecraft heat pipes. The basic test goals for the OAO heat pipes are similar to the test goals for other heat pipe systems, and therefore only the OAO pipes are discussed.

Test Results

Long Periods for Temperature Stabilization. One of the first and most noticeable differences realized under the thermal-vacuum testing of the two high-power OAO-C pipes was the length of time required to stabilize the pipes. Thermal-vacuum stabilization periods were on the order of four to six times as long as bench testing times.

Higher Delta Temperatures. A second difference was that the delta temperatures (ΔT 's) recorded during vacuum-testing were higher than those recorded on the bench. This was probably due to convection on the bench, even though the pipes during the bench testing were wrapped in 10 layers of super-insulation. Since tilt tests were performed and the data were carefully recorded, good accuracy as to stabilization points was achieved.

Effects of Tilt. It was noticed that the overall pipe ΔT 's were lower at a 1/4-inch tilt (the evaporator always above the condenser) than at the level test condition. This occurred in approximately 70% of all test conditions. This may be due to the effects of hydrodynamic puddling on the fluid flow, but more testing on other heat pipes is required to confirm this conclusion. This problem will be investigated further during the testing of the ATS-F pipes at Goddard.

Burnout. It was also demonstrated that as the tilt was increased, the ΔT 's in general changed very little up to the point of burnout, and in most cases there was no indication prior to burnout that the pipe would cease to function. This indicated that the wick design is excellent, and that the wick is capable of carrying large heat loads without large thermal gradients. Burnout occurs when the wicking structure in the heat-input area finally becomes unable to supply fluid as fast as it is evaporated, which causes the heat input area to become dry and the local temperature to start a rapid rise. A typical example of this sudden burnout condition is shown in table 1. For this test the chamber was under vacuum, the chamber walls were at -40°C , and the condenser was conditioned by the heat-removal unit at -55°C . Looking at the overall pipe ΔT 's in column 4 of table 1, it will be noted that little if any change was recorded as the tilt was increased. Table 1 gives the result of the thermal-vacuum test of the OAO-C

Table 1

FLIGHT-HEATER DATA

Chamber Walls at -40°C; Condensers at -55°C			
Heater Power Watts	Pipe Tilt, Inches	Pipe Average Temperature (°C)	$\Delta T(^{\circ}\text{C})$
25	0	-42.0	0.4
50	0	-37.0	1.0
75	0	-32.0	1.0
25	1/4	-40.0	0.4
50	1/4	-35.5	1.0
75	1/4	-29.5	1.0
25	1/2	-41.0	0.4
50	1/2	-35.0	1.3
75	1/2	-29.0	1.0
25	3/4	-41.5	1.0
50	3/4	-37.0	1.0 ¹
75	3/4	-	*
Chamber Walls at -40°C; Condensers at -40°C			
50	1/2	-24.5	1.2
50	3/4	-24.0	1.1
75	3/4	-18.0	1.6
25	1	-27.5	0.5
50	1	-23.5	3.0
75	1	-16.0	3.0 ²

ΔT = Temperature difference between evaporator and condenser sections.

*Burnout: Interior wall becomes dry due to heating rate exceeding the fluid return rate.

¹Pipe was allowed to reprime and burnout recurred under the same test conditions.

²Theoretical ΔT limit approached.

spiral artery heat pipe, when only the flight heaters were used. Highlighting the importance of the heat removal effects, it will be noted that there was a considerable difference in pipe performance when the condensers were changed from -55°C to -40°C, also shown in table 1. This indicates that under some test conditions the condenser temperature is the controlling factor.

Burnout, in which one section of the pipe becomes very hot, was also characterized during the tests by the remaining portions of the pipe becoming slightly cooler, since the heat-removal mechanism continually removed heat from the fluid and vapor near the condenser.

Once burnout has occurred, the heat pipe must show the ability to reprime (Ref. 27). The technique used during the tests at Goddard to restore the pipe to proper functioning after burnout is as follows: If the pipe is in a tilted position when burnout occurs, all power is turned off, and the pipe is allowed to recover in this position. After low ΔT 's, approximately 1° to 2°C, have been established the pipe is releveled, and is allowed to remain in this position for approximately 30 minutes. In all the burnout cases tested so far, this has worked. When the pipe is left in a tilted position, this permits the formation of gas bubbles and makes it easier for them to dissolve. As the liquid inches up the pipe it tends to form trapped gas pockets, which are lighter than the liquid, and these gas pockets are pushed from the colder toward the warmer areas, allowing them to condense or dissolve.

On the other hand, if a large gas pocket is trapped when the pipe is in the level position, it may be overwhelmed by a large amount of fluid, and then the pipe will require a lengthy recovery time, since some noncondensable gases, such as hydrogen, may be present and trapped. This situation would result in a partial recovery only, and it causes poor thermal performance, i. e., large ΔT 's. The tilted recovery method is used also because the pipes must be able to reprime in their burnout positions, to indicate the ability of the pipe to function properly in a 1-g field and in space.

Cool-out and Overheating. Two other types of failures also occurred during testing. The first type is denoted as a cool-out, and the second as overheating. A cool-out occurs when the heat pipe is working well, i. e., with low ΔT 's. As the heater power is increased to high limits, using the test heaters only, and while the tilt on the pipe is increased, as shown in table 2, fluid collects in the colder portions of the pipe, causing a local cold spot in the pipe. Thus while the pipe is working well a large gradient can occur in the condenser section of the pipe, causing an out-of-tolerance condition.

This cool-out can occur in more than one location if more than one heat rejection area (condenser) is being used. This results in stable pipe temperatures but with high thermal gradients. When the pipe was left in this stable, cool-out condition for several hours it showed no signs of burnout or change.

Overheating, on the other hand, occurs at elevated temperatures. What happens in a case like this is that the fluid heat transfer property begins to

Table 2

TEST-HEATER DATA

Chamber Walls at -40°C; Condensers at -40°C			
Heater Power per Saddle, Watts	Pipe Tilt, Inches	Pipe Average Temperature (°C)	ΔT (°C)
5	0	-35.0	0.5
15	0	-32.0	0.8
25	0	-30.5	0.8
35	0	-29.0	1.3
40	0	-26.0	3.0
70	3/4	12.0	6.0
80	3/4	17.0	8.0
10	1	-27.0	2.0
30	1	-13.0	3.5
50	1	0.0	4.0
70	1	11.5	8.0 ¹
80	1	16.5	16.5 ¹

¹High ΔT caused by condenser cooling dropout, not by overheating.

wane, i.e., the ability of the fluid to carry large heat loads diminishes greatly. Thus the temperature of the heat pipe in the evaporator section becomes higher than the rest of the heat pipe. This is distinctly different from burnout, which is characterized by a local highly-elevated temperature in the evaporator section of the heat pipe while the remaining evaporator area of the heat pipe remains relatively cool.

There is no way to distinguish between these two conditions without careful analysis of the data. Thus when ΔT test data is recorded, it is necessary to denote the reason for large ΔT 's.

Effect of Environment. Tables 3 and 4 show that even for a good heat pipe system the environment does have some affect on the overall pipe performance, as shown by the slightly higher ΔT 's as the overall pipe temperature is elevated by its environment.

The typical test results given in tables 1 to 4 show that high-powered pipes with low ΔT 's can be built, and these heat pipes can aid in the isothermalization

Table 3

FLIGHT-HEATER DATA

Chamber Walls at 0°C; Condenser at 0°C			
Heater Power, Watts	Pipe Tilt, Inches	Pipe Average Temperature (°C)	ΔT (°C)
25	0	9.0	1.0
50	0	14.0	1.0
75	0	20.1	1.0
25	1/4	8.5	0.5
50	1/4	14.0	0.5
75	1/4	19.0	0.5
25	1/2	9.0	0.5
50	1/2	14.5	1.0
75	1/2	20.2	0.9
25	3/4	10.0	0.1
50	3/4	14.8	0.6
75	3/4	21.0	1.2
25	1	9.6	0.4
50	1	15.0	1.2
75	1	21.1	1.8

of spacecraft components in gravitational fields, and should function better under zero-gravity conditions.

Table 4

FLIGHT-HEATER DATA

Chamber Walls at +20°C; Condenser at +20°C			
Heater Power, Watts	Pipe Tilt, Inches	Pipe Average Temperature (°C)	$\Delta T(^{\circ}\text{C})$
25	0	28.0	0.7
50	0	32.0	0.7
75	0	37.1	0.9
25	1/4	27.2	0.5
50	1/4	31.6	0.9
75	1/4	37.3	0.7
25	1/2	28.0	0.6
50	1/2	32.4	0.8
75	1/2	37.1	0.9
25	3/4	28.0	0.4
50	3/4	32.7	1.0
75	3/4	38.3	1.5
25	1	28.0	0.9
50	1	32.0	1.9
75	1	36.9	2.1

REFERENCES

1. Eastman, G. Yale. "The Heat Pipe." Scientific American, 218, 5, p. 38ff. May 1968.
2. Grover, G. M., et. al. "Structures of Very High Thermal Conductance." J. Appl. Phys. 35, 1990 (1964).
3. Feldman and Whiting. "The Heat Pipe." Mechanical Engineering, February, 1967.
4. Feldman and Whiting. "Applications of the Heat Pipe." Mechanical Engineering, November, 1968.
5. Turner, R. C. "The Constant Temperature Heat Pipe - A Unique Device for the Thermal Control of Spacecraft Components." AIAA 4th Thermophysics Conference, June 1969.
6. Abramsom, Norman H. The Dynamic Behavior of Liquids in Moving Containers. NASA SP-106, 1966.
7. Waters, E. D. "Design, Fabrication, and Testing of ATS-E Solar Panel/Heat Pipe Substrates." Summary Report for NASA, DAC-63370, June 1969.
8. Hall, W. B. "Heat Pipe Experiments." Radio Corporation of America.
9. Cotter, T. P. "Theory of Heat Pipes." Los Alamos Publication LA-3246-MS, March, 1965.
10. Cotter, T. P. "Heat Pipe Startup Dynamics." Thermionic Conversion Specialist Conference, Palo Alto, California, October, 1967.
11. Kemme, J. E. "High Performance Heat Pipes." Thermionic Conversion Specialist Conference, October, 1967.
12. Katzoff, S. "Heat Pipes and Vapor Chambers for Thermal Control of Spacecraft." AIAA Paper No. 67-310, April 20, 1967.
13. Katzoff, S. "Notes on Heat Pipes and Vapor Chambers and Their Application to Thermal Control of Spacecraft." NASA, Langley Research Center Paper No. 67-26796.

Preceding page blank

14. Kemme, J. E. "Heat Pipe Capability Experiments." Los Alamos Publication LA-3585-MS, October, 1966.
15. McAdams, William H. Heat Transmission. Third Edition McGraw Hill Book Co., 1954.
16. Anderson, J. L., and Lantz, E. "A Nuclear Thermionic Space Power Concept Using Rod Control and Heat Pipes." NASA TN D-5250, May, 1969.
17. Arcella, F. G., and Dzakowic, G. S. "Heat Pipe Function Isothermally and Adaptably." Research and Design Trend, August, 1969.
18. Kemme, J. E. "Heat Pipe Design Considerations." Los Alamos Publication LA-4221-MS, August 1, 1969.
19. Anand, D. K. "On the Performance of a Heat Pipe." Engineering Notes, December, 1965.
20. Jakob, Max. Heat Transfer. New York, John Wiley & Sons, 1949. Vols. I, II.
21. Cotter, T. P. "Heat Pipe Startup Dynamics." Thermionic Conversion Specialist Conference, October, 1967.
22. Lamb, Sir Horace. Hydrodynamics. New York, Dover Publication, 1932.
23. Gerrels, E. E., and Larson, J. W. "Brayton Cycle Vapor Chamber (Heat Pipe) Radiator Study." NASA CR-1677, February 1971.
24. Marshburn, J. P. "Results of Thermal Vacuum Testing the OAO-C Dynatherm Heat Pipe." GSFC Memorandum, February, 1971.
25. Marshburn, J. P. "Results of Thermal-Vacuum Testing of the Grumman OAO-C Structural Heat Pipe." GSFC Memorandum, November, 1971.
26. Marshburn, J. P. "Test of the Redesigned Level-6 Grumman Spiral-Artery Heat Pipe Under Thermal-Vacuum Conditions." GSFC Memorandum, December, 1971.
27. Goddard Space Flight Center. Specification OB-A-0086-C. OAO-C Heat Pipe. September 18, 1970.